Available on-line at www.prace-ri.eu

Partnership for Advanced Computing in Europe

Hybrid Total FETI Method

T. Kozubek[a,*], M. Jarošová[a], M. Menšík[a], A. Markopoulos[a]

[a]CE IT4Innovations, VSB-TU of Ostrava, 17. listopadu 15, 70833 Ostrava, Czech Republic

Abstract

We describe a hybrid FETI (Finite Element Tearing and Interconnecting) method based on our variant of the FETI type domain decomposition method called Total FETI. In our approach a small number of neighboring subdomains is aggregated into the clusters, which results into a smaller coarse problem. To solve the original problem the Total FETI method is applied twice: to the clusters (macro-subdomains) and then to the subdomains in each cluster. This approach simplifies implementation of hybrid FETI methods and enables to extend parallelization of the original problem up to tens of thousands of cores due to the coarse space reduction and thus lower memory requirements. The performance is demonstrated on a linear elasticity benchmark.

Keywords Domain decomposition, Total FETI, Hybrid FETI, scalable algorithm.

1. Introduction

The goal of this paper is to describe a hybrid FETI method based on our variant of the FETI type domain decomposition method called Total FETI [5]. The original FETI method, also called FETI-1 method, was originally introduced for the numerical solution of the large linear systems arising in linearized engineering problems by Farhat and Roux [1]. In both FETI methods a body is decomposed into several non-overlapping subdomains and the continuity between the subdomains is enforced by Lagrange multipliers. Using a theory of duality, a smaller and relatively well conditioned dual problem can be derived and efficiently solved by suitable variant of the conjugate gradient algorithm.

The original FETI algorithm, where only the favorable distribution of the spectrum of the dual Schur complement matrix [2] was considered, was efficient only for a small number of subdomains. So it was later extended by introducing a natural coarse problem [3, 4], whose solution was implemented by auxiliary projectors so that the resulting algorithm became in a sense optimal [3, 4].

In the Total FETI method [5] also the Dirichlet boundary conditions are enforced by Lagrange multipliers. Hence all subdomain stiffness matrices are singular with à-priori known kernels which is a great advantage in the numerical solution. With a known kernel basis we can regularize effectively the stiffness matrix [6, 13] and use any standard Cholesky type decomposition method for nonsingular matrices.

Even if, there are several efficient coarse problem parallelization strategies [7], still there are size limitations of the coarse problem. So several hybrid (multilevel) methods were proposed [9, 8]. The key idea is to aggregate a small number of neighboring subdomains into the clusters, which naturally results into a smaller coarse problem. In our Hybrid Total FETI, the aggregation of subdomains into clusters is enforced again by Lagrange multipliers. Thus the Total FETI method is used on both cluster and subdomain levels. This approach simplifies implementation of hybrid FETI methods and enables to extend parallelization of the original problem up to tens of thousands of cores due to lower memory requirements. The positive effect is a reduction of the coarse space, the negative one is worse convergence rate compared with the original TFETI. To improve it the transformation of the basis originally introduced by Klawonn and Widlund [11], Klawonn and Rheinbach [10], and Li and Widlund [12] is applied to the derived hybrid algorithm.

The paper is organized as follows. After introducing a model problem in Section 2, we describe Hybrid Total FETI method (H-TFETI) in Section 3. The transformation of basis is briefly described and applied to the derived hybrid algorithm in Section 4. The results of numerical experiments are illustrated in Section 5.

2. The model problem

Let us consider a model problem from the linear elasticity. The isotropic elastic body occupies a domain $\Omega \subset \mathbb{R}^d, d = 2, 3$, with the sufficiently smooth boundary Γ. We suppose that its nonempty part $\Gamma_{\mathbf{U}}$ is fixed,

*Corresponding author.
tel. +420 597 323 494 fax. +420 596 919 597 e-mail. tomas.kozubek@vsb.cz

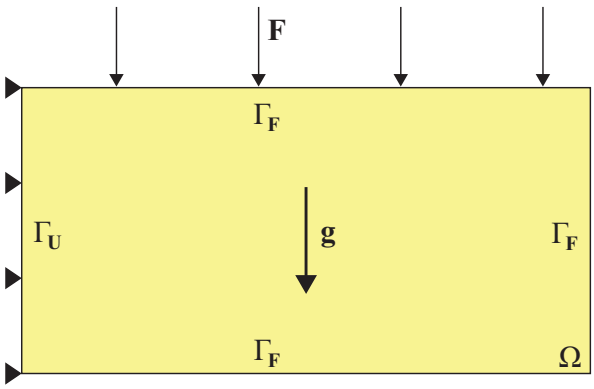

Fig. 1. Model problem

so the homogeneous Dirichlet boundary condition is used here and the rest of the boundary $\Gamma_{\mathbf{F}} = \Gamma \backslash \overline{\Gamma}_{\mathbf{U}}$ is under the action of the external forces $\mathbf{F}$, so the Neumann boundary condition is considered (see Figure 1). Generalization to other boundary conditions (symmetry, periodic) is without any complications.

Let $c_{ijk\ell} : \Omega \to \mathbb{R}$ and $\mathbf{g} : \Omega \to \mathbb{R}^d$ denote the entries of the symmetric elliptic elasticity tensor and a vector of body forces, respectively. For any sufficiently smooth displacement $\mathbf{u} : \overline{\Omega} \to \mathbb{R}^d$, the total potential energy is defined by

$$J(\mathbf{u}) = \frac{1}{2}a(\mathbf{u},\mathbf{u}) - \int_\Omega \mathbf{g}^\top \mathbf{u}\, d\Omega - \int_{\Gamma_F} \mathbf{F}^\top \mathbf{u}\, d\Gamma, \tag{1}$$

where

$$a(\mathbf{u},\mathbf{v}) = \int_\Omega c_{ijk\ell} e_{ij}(\mathbf{u}) e_{k\ell}(\mathbf{v}) d\Omega \quad \text{and} \quad e_{k\ell}(\mathbf{u}) = \frac{1}{2}\left(\frac{\partial u_k}{\partial x_\ell} + \frac{\partial u_\ell}{\partial x_k}\right). \tag{2}$$

Let us introduce the Sobolev space

$$W = \{\mathbf{v} \in H^1(\Omega)^d : \ \mathbf{v} = \mathbf{u} \ \text{ on } \ \Gamma_U\}.$$

The displacement $\mathbf{u} \in W$ of the body in equilibrium satisfies

$$J(\mathbf{u}) \leq J(\mathbf{v}) \quad \text{for any} \quad \mathbf{v} \in W. \tag{3}$$

Under our assumptions J is coercive that guarantees the existence and the uniqueness of the solution to (3).

We will discretize our problem by low order, conforming finite elements. Let us consider suitable 2D rectangular discretization of Ω with a discretization parameter h and denote by $W^h \subset W$ the corresponding finite element space. The associate discrete problem is then to find $\mathbf{u}^h \in W^h$, such that

$$J(\mathbf{u}^h) \leq J(\mathbf{v}^h) \quad \text{for any} \quad \mathbf{v}^h \in W^h. \tag{4}$$

Hereafter, we will drop the subscript h.

3. Hybrid Total FETI

To apply the H-TFETI approach to solve problem (4) we first of all tear the body from the part of the boundary with the Dirichlet boundary condition as in the Total FETI approach. Then we decompose the body into clusters and the clusters into subdomains, see Fig. 2. Finally, we introduce new "gluing" conditions on the subdomain interfaces to ensure the continuity of the solution and on the boundaries with imposed Dirichlet data.

Let domain Ω be decomposed into N_c relatively large non-overlapping clusters of diameter H_c and let each cluster be decomposed into N_s all floating non-overlapping subdomains of diameter H_s. The total number of subdomains is then $N = N_c \times N_s$. To ensure the continuity of the displacements and of their normal derivatives across the interface we have to introduce so called gluing conditions.

The resulting quadratic programming (QP) problem reads as

$$\min_{\mathbf{u}} \frac{1}{2}\mathbf{u}^\top \mathbf{K}\mathbf{u} - \mathbf{f}^\top \mathbf{u} \quad \text{subject to} \quad \mathbf{B}\mathbf{u} = \mathbf{c}, \tag{5}$$

where

$$\mathbf{K} = \begin{bmatrix} \mathbf{K}^1 & & & \\ & \mathbf{K}^2 & & \\ & & \ddots & \\ & & & \mathbf{K}^N \end{bmatrix} \tag{6}$$

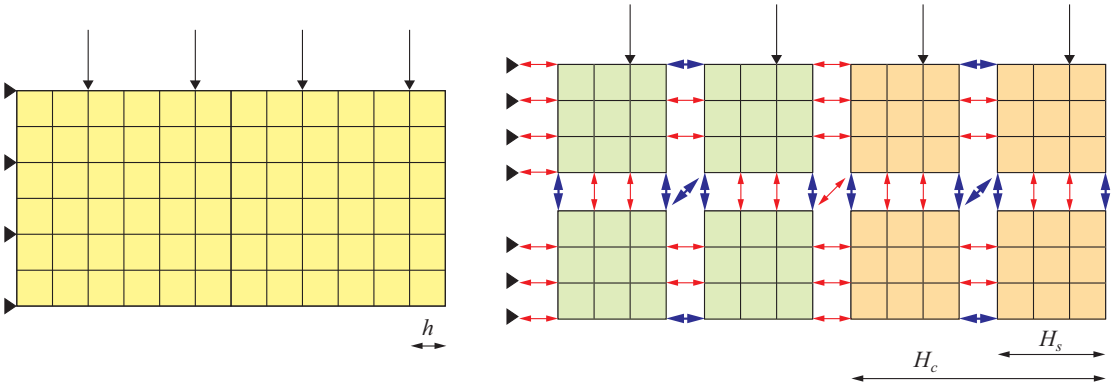

Fig. 2. Hybrid TFETI domain decomposition.

denotes a symmetric positive semidefinite stiffness matrix of order n, $\mathbf{B}$ denotes an $m \times n$ full rank constraint matrix, $\mathbf{f} \in \mathbb{R}^n$ is a load vector, and $\mathbf{c} \in \mathbb{R}^m$ is a constraint vector.

The fact that the blocks $\mathbf{K}^i$ corresponding to Ω^i are positive semidefinite sparse matrices with kernel bases à-priori known enables us to regularize each block and then decompose it efficiently using the standard (sparse) Cholesky factorization for non-singular matrices [13, 14]. The load vector $\mathbf{f}$ describes the nodal forces arising from the volume forces and/or some other imposed traction.

The matrix $\mathbf{B} = [\mathbf{B}_g^\top,\ \mathbf{B}_D^\top]^\top \in \mathbb{R}^{m \times n}$ also called jump operator and the vector $\mathbf{c} = [\mathbf{o}^\top, \mathbf{c}_D^\top]^\top$ enforce the continuity at the interface variables and the Dirichlet data. Typically m, the number of Lagrange multipliers, is much smaller than n, the number of degrees of freedom. The matrix $\mathbf{B}$ is constructed using values $\{-1, 0, 1\}$ in such a way, that the values of the solution $\mathbf{u}$ associated with more than one subdomain coincide when $\mathbf{B}_g\mathbf{u} = \mathbf{o}$ and the values of the solution $\mathbf{u}$ on the boundary with the Dirichlet condition satisfy $\mathbf{B}_D\mathbf{u} = \mathbf{c}_D$. Let us note that $\mathbf{B}$ can be directly assembled to have orthonormal rows only by special treating of the rows of $\mathbf{B}$ corresponding to the nodes shared by more than two subdomains.

The problem (5) has the same structure as in standard Total FETI method and could be solved by this standard approach. However, to describe the H-TFETI method, we will consider the problem (5) in the form

$$\min \frac{1}{2}\mathbf{u}^\top \mathbf{K}\mathbf{u} - \mathbf{u}^\top \mathbf{f} \quad \text{subject to} \quad \left\{ \begin{array}{l} \mathbf{B}_0\mathbf{u} = \mathbf{c}_0 \\ \mathbf{B}_1\mathbf{u} = \mathbf{c}_1 \end{array} \right. , \tag{7}$$

where the equality constraints are split up into two parts. The first part $\mathbf{B}_0\mathbf{u} = \mathbf{c}_0 := \mathbf{o}$ consists of m_0 equalities enforcing the continuity in the subdomain corner nodes of each cluster, while $\mathbf{B}_1\mathbf{u} = \mathbf{c}_1$ consists of m_1 equalities enforcing the continuity across the rest of the subdomain interfaces and the Dirichlet condition.

The KKT optimality conditions lead to the saddle point problem

$$\left[\begin{array}{ccc|c} \mathbf{K} & \mathbf{B}_0^\top & \mathbf{B}_1^\top & \mathbf{u} \\ \mathbf{B}_0 & \mathbf{O} & \mathbf{O} & \boldsymbol{\lambda}_0 \\ \hline \mathbf{B}_1 & \mathbf{O} & \mathbf{O} & \boldsymbol{\lambda}_1 \end{array}\right] = \left[\begin{array}{c} \mathbf{f} \\ \mathbf{c}_0 \\ \hline \mathbf{c}_1 \end{array}\right] \tag{8}$$

or

$$\left[\begin{array}{c|c} \tilde{\mathbf{K}} & \tilde{\mathbf{B}}^\top \\ \hline \tilde{\mathbf{B}} & \mathbf{O} \end{array}\right] \left[\begin{array}{c} \tilde{\mathbf{u}} \\ \hline \tilde{\boldsymbol{\lambda}} \end{array}\right] = \left[\begin{array}{c} \tilde{\mathbf{f}} \\ \hline \tilde{\mathbf{c}} \end{array}\right], \tag{9}$$

where $\tilde{\mathbf{K}}, \tilde{\mathbf{B}}, \tilde{\mathbf{u}}, \tilde{\boldsymbol{\lambda}}, \tilde{\mathbf{f}}$, and $\tilde{\mathbf{c}}$ respect the block structure indicated in (8).

The first equation of the system (9) has a solution iff

$$\tilde{\mathbf{f}} - \tilde{\mathbf{B}}^\top \tilde{\boldsymbol{\lambda}} \in \mathrm{Im}\tilde{\mathbf{K}}, \tag{10}$$

which can be expressed more conveniently by means of a matrix $\tilde{\mathbf{R}}$ whose columns span the null space of $\tilde{\mathbf{K}}$ as

$$\tilde{\mathbf{R}}^\top(\tilde{\mathbf{f}} - \tilde{\mathbf{B}}^\top \tilde{\boldsymbol{\lambda}}) = \mathbf{o}, \tag{11}$$

where

$$\tilde{\mathbf{R}} = \begin{bmatrix} \mathbf{R}_c^1 & & \\ & \ddots & \\ & & \mathbf{R}_c^{N_c} \\ \mathbf{O} & \mathbf{O} & \mathbf{O} \end{bmatrix} \quad \text{and} \quad \mathbf{R}_c^i = \begin{bmatrix} \mathbf{R}^{1,i} \\ \vdots \\ \mathbf{R}^{N_s,i} \end{bmatrix}, \tag{12}$$

with $\mathbf{R}^{p,i}$, $p = 1, \ldots, N_s$ meaning the pth subdomain of the ith cluster. As the kernel bases of the subdomains are known à-priori, the blocks $\mathbf{R}^{p,i}$ may be assembled directly from the segments $\mathbf{R}_k$ defined for the kth mesh

node as follows

$$\mathbf{R}_k = \begin{bmatrix} 1 & 0 & -y_k \\ 0 & 1 & x_k \end{bmatrix} \text{ in 2D} \quad \text{and} \quad \mathbf{R}_k = \begin{bmatrix} 1 & 0 & 0 & 0 & -z_k & y_k \\ 0 & 1 & 0 & z_k & 0 & -x_k \\ 0 & 0 & 1 & -y_k & x_k & 0 \end{bmatrix} \text{ in 3D.} \tag{13}$$

In order to eliminate the primal variables $\tilde{\mathbf{u}}$ from the singular system given by the first equation in (9) we use a generalized inverse matrix $\tilde{\mathbf{K}}^+$ to $\tilde{\mathbf{K}}$ satisfying $\tilde{\mathbf{K}}\tilde{\mathbf{K}}^+\tilde{\mathbf{K}} = \tilde{\mathbf{K}}$. It may be easily verified that if $\tilde{\mathbf{u}}$ is a solution to the first equation of (9), then there exists a vector $\tilde{\boldsymbol{\alpha}}$ such that

$$\tilde{\mathbf{u}} = \tilde{\mathbf{K}}^+(\tilde{\mathbf{f}} - \tilde{\mathbf{B}}^\top\tilde{\boldsymbol{\lambda}}) + \tilde{\mathbf{R}}\tilde{\boldsymbol{\alpha}}. \tag{14}$$

Substituting (14) into the second equation of (9) and using (11), we get

$$\begin{bmatrix} \tilde{\mathbf{B}}\tilde{\mathbf{K}}^+\tilde{\mathbf{B}}^\top & -\tilde{\mathbf{B}}\tilde{\mathbf{R}} \\ -\tilde{\mathbf{R}}^\top\tilde{\mathbf{B}}^\top & \mathbf{O} \end{bmatrix} \begin{bmatrix} \tilde{\boldsymbol{\lambda}} \\ \tilde{\boldsymbol{\alpha}} \end{bmatrix} = \begin{bmatrix} \tilde{\mathbf{B}}\tilde{\mathbf{K}}^+\tilde{\mathbf{f}} - \tilde{\mathbf{c}} \\ -\tilde{\mathbf{R}}^\top\tilde{\mathbf{f}} \end{bmatrix}. \tag{15}$$

Let us introduce the new notation

$$\begin{array}{ll} \tilde{\mathbf{F}} = \tilde{\mathbf{B}}\tilde{\mathbf{K}}^+\tilde{\mathbf{B}}^\top, & \tilde{\mathbf{g}} = \tilde{\mathbf{B}}\tilde{\mathbf{K}}^+\tilde{\mathbf{f}} - \tilde{\mathbf{c}}, \\ \tilde{\mathbf{G}} = -\tilde{\mathbf{R}}^\top\tilde{\mathbf{B}}^\top, & \tilde{\mathbf{e}} = -\tilde{\mathbf{R}}^\top\tilde{\mathbf{f}}, \end{array}$$

so that the system (15) reads as

$$\begin{bmatrix} \tilde{\mathbf{F}} & \tilde{\mathbf{G}}^\top \\ \tilde{\mathbf{G}} & \mathbf{O} \end{bmatrix} \begin{bmatrix} \tilde{\boldsymbol{\lambda}} \\ \tilde{\boldsymbol{\alpha}} \end{bmatrix} = \begin{bmatrix} \tilde{\mathbf{g}} \\ \tilde{\mathbf{e}} \end{bmatrix}. \tag{16}$$

As in standard TFETI we introduce orthogonal projector $\tilde{\mathbf{P}} = \mathbf{I} - \tilde{\mathbf{G}}^\top(\tilde{\mathbf{G}}\tilde{\mathbf{G}}^\top)^{-\mathbf{1}}\tilde{\mathbf{G}}$ onto the kernel of $\tilde{\mathbf{G}}$. Applying $\tilde{\mathbf{P}}$ to (16) we get

$$\tilde{\mathbf{P}}\tilde{\mathbf{F}}\tilde{\boldsymbol{\lambda}} = \tilde{\mathbf{P}}\tilde{\mathbf{g}} \quad \text{subject to} \quad \tilde{\mathbf{G}}\tilde{\boldsymbol{\lambda}} = \tilde{\mathbf{e}} \tag{17}$$

and after homogenization of the constraints we get

$$\tilde{\mathbf{P}}\tilde{\mathbf{F}}\tilde{\boldsymbol{\lambda}}_{\mathrm{Ker}} = \tilde{\mathbf{P}}(\tilde{\mathbf{g}} - \tilde{\mathbf{F}}\tilde{\boldsymbol{\lambda}}_{\mathrm{Im}}) \quad \text{for} \quad \tilde{\boldsymbol{\lambda}}_{\mathrm{Ker}} \in \mathbf{Ker}\tilde{\mathbf{G}}, \tag{18}$$

where $\tilde{\boldsymbol{\lambda}}_{\mathrm{Im}} = \tilde{\mathbf{G}}^\top(\tilde{\mathbf{G}}\tilde{\mathbf{G}}^\top)^{-\mathbf{1}}\tilde{\mathbf{e}}$ and $\tilde{\boldsymbol{\lambda}} = \tilde{\boldsymbol{\lambda}}_{\mathrm{Ker}} + \tilde{\boldsymbol{\lambda}}_{\mathrm{Im}}$.

Lemma 1 *The matrix* $\tilde{\mathbf{P}}\tilde{\mathbf{F}}$ *is symmetric positive definite on* $\mathrm{Ker}\tilde{\mathbf{G}}$.

Proof Let $\boldsymbol{\mu} \in \mathrm{Ker}\tilde{\mathbf{G}}$. Then $\mathbf{o} = \tilde{\mathbf{G}}\boldsymbol{\mu} = -\tilde{\mathbf{R}}^\top\tilde{\mathbf{B}}^\top\boldsymbol{\mu} = -\tilde{\mathbf{R}}^\top\mathbf{v}$, where $\mathbf{v} = \tilde{\mathbf{B}}^\top\boldsymbol{\mu}$. Hence $\mathbf{v} \in \mathrm{Im}\tilde{\mathbf{B}}^\top \cap \mathrm{Im}\tilde{\mathbf{K}}$. It is enough to show that $\sigma_{\min}(\tilde{\mathbf{P}}\tilde{\mathbf{F}}|_{\mathrm{Ker}\tilde{\mathbf{G}}}) > 0$, where $\sigma_{\min}(\mathbf{X})$ denotes the smallest eigenvalue of $\mathbf{X}$. We get

$$\sigma_{\min}(\tilde{\mathbf{P}}\tilde{\mathbf{F}}|_{\mathrm{Ker}\tilde{\mathbf{G}}}) = \min_{\substack{\boldsymbol{\mu}\in\mathrm{Ker}\tilde{\mathbf{G}} \\ \boldsymbol{\mu}\neq\mathbf{o}}} \frac{\boldsymbol{\mu}^\top\tilde{\mathbf{P}}\tilde{\mathbf{F}}\boldsymbol{\mu}}{\boldsymbol{\mu}^\top\boldsymbol{\mu}} = \min_{\substack{\boldsymbol{\mu}\in\mathrm{Ker}\tilde{\mathbf{G}} \\ \boldsymbol{\mu}\neq\mathbf{o}}} \frac{\boldsymbol{\mu}^\top\tilde{\mathbf{B}}\tilde{\mathbf{K}}^+\tilde{\mathbf{B}}^\top\boldsymbol{\mu}}{\boldsymbol{\mu}^\top\tilde{\mathbf{B}}\tilde{\mathbf{B}}^\top\boldsymbol{\mu}} \cdot \frac{\boldsymbol{\mu}^\top\tilde{\mathbf{B}}\tilde{\mathbf{B}}^\top\boldsymbol{\mu}}{\boldsymbol{\mu}^\top\boldsymbol{\mu}} \tag{19}$$

$$= \min_{\substack{\mathbf{v}\in\mathrm{Im}\tilde{\mathbf{B}}^\top\cap\mathrm{Im}\tilde{\mathbf{K}} \\ \mathbf{v}=\tilde{\mathbf{B}}^\top\boldsymbol{\mu},\ \boldsymbol{\mu}\in\mathrm{Ker}\tilde{\mathbf{G}},\ \boldsymbol{\mu}\neq\mathbf{o}}} \frac{\mathbf{v}^\top\tilde{\mathbf{K}}^+\mathbf{v}}{\mathbf{v}^\top\mathbf{v}} \cdot \frac{\boldsymbol{\mu}^\top\tilde{\mathbf{B}}\tilde{\mathbf{B}}^\top\boldsymbol{\mu}}{\boldsymbol{\mu}^\top\boldsymbol{\mu}} > 0 \tag{20}$$

using $\boldsymbol{\mu}^\top\tilde{\mathbf{P}}\tilde{\mathbf{F}}\boldsymbol{\mu} = \boldsymbol{\mu}^\top\tilde{\mathbf{F}}\boldsymbol{\mu}$ for $\boldsymbol{\mu} \in \mathrm{Ker}\tilde{\mathbf{G}}$, $\tilde{\mathbf{B}}\tilde{\mathbf{B}}^\top = \mathbf{I}$, and the fact that $\mathbf{v}^\top\tilde{\mathbf{K}}^+\mathbf{v}$ is independent of the choice of $\tilde{\mathbf{K}}^+$ iff $\mathbf{v} \in \mathrm{Im}\tilde{\mathbf{K}}$. The symmetry is obvious. ■

Because of Lemma 1 the problem (18) may be solved efficiently by the PCGP (Preconditioned Conjugate Gradient with Projectors) algorithm.

In every PCGP iteration we need to compute $\tilde{\mathbf{x}} = \tilde{\mathbf{K}}^+\tilde{\mathbf{b}}$, where $\tilde{\mathbf{b}}$ is a given vector. To do this we solve the system

$$\tilde{\mathbf{K}}\tilde{\mathbf{x}} = \tilde{\mathbf{b}} \quad \Longleftrightarrow \quad \begin{bmatrix} \mathbf{K} & \mathbf{B}_0^\top \\ \mathbf{B}_0 & \mathbf{O} \end{bmatrix} \begin{bmatrix} \mathbf{x}_0 \\ \boldsymbol{\mu}_0 \end{bmatrix} = \begin{bmatrix} \mathbf{b}_0 \\ \mathbf{d}_0 \end{bmatrix} \tag{21}$$

by a TFETI based solver again. Using

$$\mathbf{x}_0 = \mathbf{K}^+(\mathbf{b}_0 - \mathbf{B}_0^\top\boldsymbol{\mu}_0) + \mathbf{R}_0\boldsymbol{\beta}_0, \tag{22}$$

and substituting it into the second equation in (21) we get

$$\begin{bmatrix} \mathbf{F}_0 & \mathbf{G}_0^\top \\ \mathbf{G}_0 & \mathbf{O} \end{bmatrix} \begin{bmatrix} \boldsymbol{\mu}_0 \\ \boldsymbol{\beta}_0 \end{bmatrix} = \begin{bmatrix} \mathbf{g}_0 \\ \mathbf{e}_0 \end{bmatrix}, \tag{23}$$

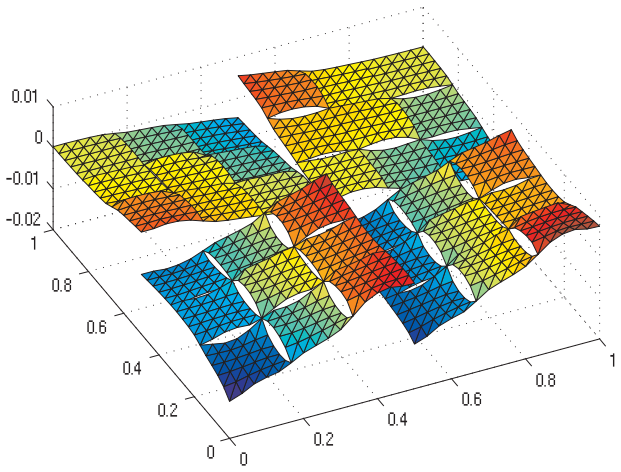

Fig. 3. Hybrid TFETI

where

$$\begin{array}{ll} \mathbf{F}_0 = \mathbf{B}_0\mathbf{K}^+\mathbf{B}_0^\top, & \mathbf{g}_0 = \mathbf{B}_0\mathbf{K}^+\mathbf{b}_0 - \mathbf{d}_0, \\ \mathbf{G}_0 = -\mathbf{R}_0^\top\mathbf{B}_0^\top, & \mathbf{e}_0 = -\mathbf{R}_0^\top\mathbf{b}_0, \end{array}$$

and

$$\mathbf{R}_0 = \begin{bmatrix} \mathbf{R}^1 & & \\ & \ddots & \\ & & \mathbf{R}^N \end{bmatrix}, N = N_c \times N_s. \tag{24}$$

We note that matrices $\mathbf{R}^j$, $j = 1, ..., N$ in (24) are the same as $\mathbf{R}^{p,i}$, $p = 1, ..., N_s$, $i = 1, ..., N_c$ in (12) with $j = (i-1)\cdot N_s + p$. To obtain the full-rank matrix $\bar{\mathbf{G}}_0 = -\bar{\mathbf{R}}_0^\top\mathbf{B}_0^\top$ we introduce the matrix $\bar{\mathbf{R}}_0$, which is obtained from $\mathbf{R}_0$ by deleting the block columns corresponding to the last subdomains of all clusters.

Lemma 2 *Let* $\mathbf{K}^+ := \mathbf{K}_\rho^{-1}$ *be the symmetric positive definite generalized pseudoinverse obtained by the regularization of* $\mathbf{K}$ *introduced in [14]. Then the matrix* $\mathbf{F}_0$ *is symmetric positive definite on* $\mathbb{R}^{m_0}$.

Proof The proof follows immediatelly from the full-rank of $\mathbf{B}_0$ and the positive definiteness of the matrix $\mathbf{K}^+$.

Let $\bar{\mathbf{e}}_0 = -\bar{\mathbf{R}}_0^\top\mathbf{b}_0$. Obviously, using the above lemma and replacing $\mathbf{G}_0$ and $\mathbf{e}_0$ by $\overline{\mathbf{G}}_0$ and $\overline{\mathbf{e}}_0$ in (23) we get well defined saddle-point system which can be solved by PCGP again or because of its small size by a direct solver.

4. Transformation of the basis

As we mentioned reducing the coarse problem leads to a worse convergence rate of our method. To improve it we can use the transformation of the basis originally introduced by Klawonn and Widlund [11], Klawonn and Rheinbach [10], and Li and Widlund [12]. The key idea is to modify all primal finite element basis functions on each subdomain interface within the clusters to have zero averages over the respective face except one nodal basis function which is defined as average over the respective face. An example of such a modified basis restricted to the interface is depicted in Figure 4 for the 2D scalar case. We will consider the transformation of the basis represented by an orthonormal matrix $\mathbf{T}$, which performs the desired change of the basis from the new basis to the original one over all subdomain interfaces within the clusters and does not change the remaining basis functions. Originally, this approach was implemented into the FETI-DP system [10] by modifying the stiffness matrix $\mathbf{K}$. In our alternative approach, the continuity in face average nodes is enforced again by Lagrange multipliers, i.e. we have new equality conditions in matrix $\mathbf{B}_0$.

Let us consider the saddle-point system of algebraic equations corresponding to the original QP problem (5):

$$\begin{bmatrix} \mathbf{K} & \mathbf{B}^\top \\ \mathbf{B} & \mathbf{O} \end{bmatrix} \begin{bmatrix} \mathbf{u} \\ \boldsymbol{\lambda} \end{bmatrix} = \begin{bmatrix} \mathbf{f} \\ \mathbf{c} \end{bmatrix}. \tag{25}$$

By using the transformation of the basis in the form $\mathbf{u} = \mathbf{T}\mathbf{y}$ and by multiplication of the first equation of (25) from the left by $\mathbf{T}^\top$, we obtain

$$\begin{bmatrix} \mathbf{T}^\top\mathbf{K}\mathbf{T} & \mathbf{T}^\top\mathbf{B}^\top \\ \mathbf{B}\mathbf{T} & \mathbf{O} \end{bmatrix} \begin{bmatrix} \mathbf{y} \\ \boldsymbol{\lambda} \end{bmatrix} = \begin{bmatrix} \mathbf{T}^\top\mathbf{f} \\ \mathbf{c} \end{bmatrix}. \tag{26}$$

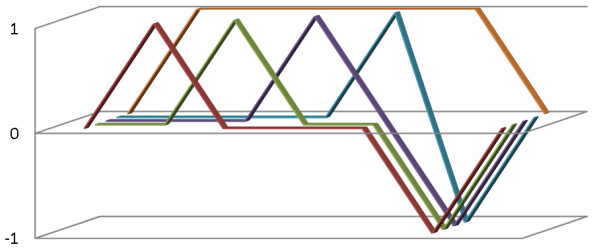

Fig. 4. Functions representing the new basis, one average basis function and basis functions with zero averages over the edge, 2D case.

Introducing the substitution $\mathbf{BT} = \mathbf{SB}$, where $\mathbf{S} = (\mathbf{BTB}^\top)(\mathbf{BB}^\top)^{-1}$, we can write

$$\begin{bmatrix} \mathbf{T}^\top\mathbf{KT} & \mathbf{B}^\top\mathbf{S}^\top \\ \mathbf{SB} & \mathbf{O} \end{bmatrix} \begin{bmatrix} \mathbf{y} \\ \boldsymbol{\lambda} \end{bmatrix} = \begin{bmatrix} \mathbf{T}^\top\mathbf{f} \\ \mathbf{c} \end{bmatrix} \tag{27}$$

or, equivalently,

$$\begin{bmatrix} \mathbf{T}^\top\mathbf{KT} & \mathbf{B}^\top \\ \mathbf{B} & \mathbf{O} \end{bmatrix} \begin{bmatrix} \mathbf{y} \\ \hat{\boldsymbol{\lambda}} \end{bmatrix} = \begin{bmatrix} \mathbf{T}^\top\mathbf{f} \\ \hat{\mathbf{c}} \end{bmatrix}, \tag{28}$$

where $\hat{\boldsymbol{\lambda}} = \mathbf{S}^\top\boldsymbol{\lambda}$ and $\hat{\mathbf{c}} = \mathbf{S}^{-1}\mathbf{c}$. The regularity of $\mathbf{S}$ is obvious. Now, it is enough to multiply the first equation by $\mathbf{T}$ and use $\mathbf{y} = \mathbf{T}^\top\mathbf{u}$ to obtain

$$\begin{bmatrix} \mathbf{K} & \mathbf{TB}^\top \\ \mathbf{BT}^\top & \mathbf{O} \end{bmatrix} \begin{bmatrix} \mathbf{u} \\ \hat{\boldsymbol{\lambda}} \end{bmatrix} = \begin{bmatrix} \mathbf{f} \\ \hat{\mathbf{c}} \end{bmatrix}. \tag{29}$$

As it was presented before, the matrix $\mathbf{B}$ can be considered in the form $\mathbf{B} = [\mathbf{B}_0^\top\ \mathbf{B}_1^\top]^\top$. The matrix $\mathbf{B}_0$ enforces the continuity in the averages (and corners), while $\mathbf{B}_1$ enforces the continuity in the remaining interface variables. Using this, we can write

$$\begin{bmatrix} \mathbf{K} & \mathbf{TB}_0^\top & \mathbf{TB}_1^\top \\ \mathbf{B}_0\mathbf{T}^\top & \mathbf{O} & \mathbf{O} \\ \mathbf{B}_1\mathbf{T}^\top & \mathbf{O} & \mathbf{O} \end{bmatrix} \begin{bmatrix} \mathbf{u} \\ \hat{\boldsymbol{\lambda}}_0 \\ \hat{\boldsymbol{\lambda}}_1 \end{bmatrix} = \begin{bmatrix} \mathbf{f} \\ \hat{\mathbf{c}}_0 \\ \hat{\mathbf{c}}_1 \end{bmatrix}. \tag{30}$$

This system has the same structure as the system (8) and can be solved in the same way. Note that, the transformation of the basis is considered only on subdomain interfaces within clusters.

5. Numerical experiments

The proposed massively parallel HTFETI algorithm was implemented in C++ using the PETSc library as a linear algebra backbone. The code was compiled by the Cray compiler with a MPI library optimized for the architecture of the HECToR supercomputer at EPCC in Edinburgh. For the scalability tests we chose a 2D linear elesticity benchmark (see Fig. 5). Particularly, we considered a steel square fixed on the left side and

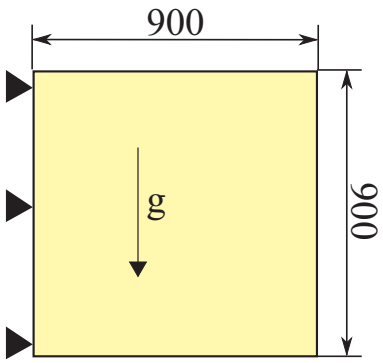

Fig. 5. Model benchmark.

deformed only by its own weight. The square was decomposed into the increasing number of subdomains with a constant number of nodes (121×121). These subdomains were organized into clusters per 16 (4×4). This

hierarchy fitted the structure of the hardware - each computing node was formed by two 16-core AMD Opteron 2.3GHz Interlagos processors. All matrices and vectors related only to the clusters are stored directly on the node occupied by that cluster. Thanks to that, all the operations inside the clusters were done in shared memory minimizing a communication overhead and the memory requirements are well distributed over the machine.

Subdomains	**DOFs***	**Iter.**	**Init. [s]**	**Sol. [s]**	**Total [s]**
400	11.712.800	115	50	46	96
1024	29.984.768	122	53	47	100
1936	56.689.952	122	53	50	103
4624	135.399.968	127	56	55	110
7744	226.759.808	127	65	61	126

Table 1. Computed results. * DOFs = degrees of freedom.

The results (see Table 6 and Fig. 6) match our original assumptions about the behaviour of the algorithm. We can notice a substantially higher number of iterations in comparison with the results of the TFETI algorithm [7] applied to the similar benchmark. This is due to the reduced coarse space working as a preconditioner. The linear loss of efficiency with rising number of used cores was partly caused by the increasing number of iterations and partly by increasing hardware overhead (execution of more instructions). On the other hand a problem with such a number of subdomains would not be possible to solve on the same machine with the original TFETI algorithm due to memory requirements on the master node.

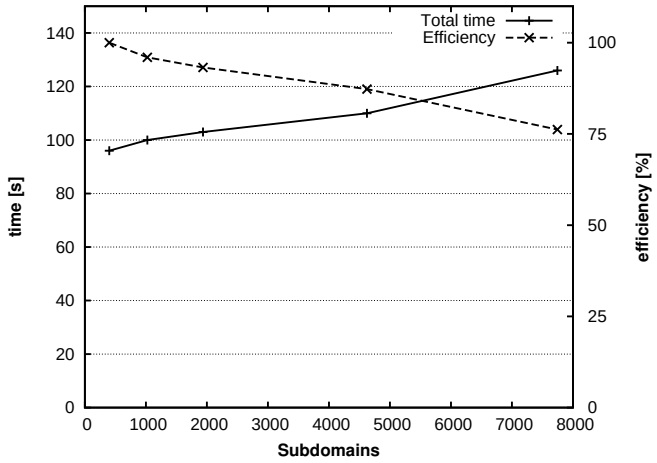

Fig. 6. Scalability behavior.

6. Conclusions

The current state of the implementation poses multiple challenges. We would like to increase its effectivity by using fast direct solvers in shared memory of clusters (such as Pardiso or MUMPS). Besides to that we are working on thorough numerical analysis of the algorithm and on the development of more efficient preconditioner. We are planning to implement the proposed method into our FLLOP (FETI Light Layer on PETSc) library [15].

7. Acknowledgments

This work was supported by the European Regional Development Fund in the IT4Innovations Centre of Excellence project (CZ.1.05/1.1.00/02.0070), by the project SPOMECH - Creating a multidisciplinary R&D team for reliable solution of mechanical problems, reg. no. CZ.1.07/2.3.00/20.0070 within Operational Programme 'Education for competitiveness' funded by Structural Funds of the European Union and state budget of the Czech Republic, and by the PRACE-2IP project receiving funding from the EU's Seventh Framework Programme (FP7/2007-2013) under grant agreement No. RI-283493.

References

1. C. Farhat, F-X. Roux, "An unconventional domain decomposition method for an efficient parallel solution of large-scale finite element systems", SIAM J. Sci. Stat. Comput. 13: 379–396, 1992.

2. F-X. Roux, “Spectral analysis of interface operator”, Proceedings of the 5th Int. Symp. on Domain Decomposition Methods for Partial Differential Equations, ed. D. E. Keyes et al., SIAM, Philadelphia 1992; 73–90.
3. C. Farhat, J. Mandel, F-X. Roux, “Optimal convergence properties of the FETI domain decomposition method”, Comput. Methods Appl. Mech. Eng. 115, 1994; 365–385.
4. F-X. Roux, C. Farhat, “Parallel implementation of direct solution strategies for the coarse grid solvers in 2-level FETI method”, Contemporary Math. 218, 1998; 158–173.
5. Z. Dostál, D. Horák, R. Kučera, “Total FETI - an easier implementable variant of the FETI method for numerical solution of elliptic PDE”, Communications in Numerical Methods in Engineering, 22(2006), 12, pp. 1155-1162
6. Z. Dostál, T. Kozubek, A. Markopoulos, M. Mensik, “Cholesky decomposition and a generalized inverse of the stiffness matrix of a floating structure with known null space”, *Applied Mathematics and Computation* 2011; **217**:6067–6077.
7. T. Kozubek, V. Vondrak, M. Mensik, D. Horak, Z. Dostal, V. Hapla, P. Kabelikova, M. Cermak, “Total FETI domain decomposition method and its massively parallel implementation”, Advances of Engeneering Software, accepted
8. A. Klawonn, O. Rheinbach, “Highly scalable parallel domain decomposition methods with an application to biomechanics”, ZAMM, 90, No. 1, pp.5-32, 2010
9. Jungho Lee: “A hybrid domain decomposition method and its applications to contact problems in mechanical engineering”, PhD thesis, New York University, 2009.
10. A. Klawonn and O. Rheinbach, “A parallel implementation of Dual-Primal FETI methods for three dimensional linear elasticity using a transformation of basis”, SIAM J. Sci. Comput., 28(5):1886–1906, 2006
11. A. Klawonn and O. B. Widlund, “Dual-primal FETI methods for linear elasticity”, Communications on pure and applied mathematics, 59(11):1523–1572, 2006
12. J. Li and O. B. Widlund, “FETI-DP, BDDC, and block Cholesky methods”, International journal for numerical methods in engineering, 66:250–271, 2006
13. T. Brzobohaty, Z. Dostal, T. Kozubek, P. Kovar, and A. Markopoulos, (2011), Cholesky decomposition with fixing nodes to stable computation of a generalized inverse of the stiffness matrix of a floating structure. Int. J. Numer. Meth. Engng., 88: 493509. doi: 10.1002/nme.3187
14. D. Horak, Z. Dostal, ”Parallelization of the Total-FETI-1 Algorithm for Contact Problems using PETSc”, in P. Ivanyi, B.H.V. Topping, (Editors), ”Proceedings of the Second International Conference on Parallel, Distributed, Grid and Cloud Computing for Engineering”, Civil-Comp Press, Stirlingshire, UK, Paper 1, 2011. doi:10.4203/ccp.95.1
15. “FLLOP Web Page”, `http://spomech.vsb.cz/feti/`